# Dye-sensitised solar cell utilising gold doped reduced graphene oxide counter electrode: influence of annealing time

*Mohd. Yusri Abd. Rahman* ✉, *Amirul Shafiq Sulaiman, Akrajas Ali Umar*

*Institute of Microengineering and Nanoelectronics (IMEN), Universiti Kebangsaan Malaysia, 43600 Bangi, Selangor, Malaysia*
✉ *E-mail: mohd.yusri@ukm.edu.my*

Published in Micro & Nano Letters; Received on 24th January 2018; Revised on 18th April 2018; Accepted on 11th May 2018

Gold doped reduced graphene oxide (rGO) films prepared via hummer method have been utilised as counter electrode of dye-sensitised solar cell. The samples were subjected to various annealing times at 120°C. The effect of annealing time on the dark current and photovoltaic performance has been investigated. The power conversion efficiency varies with annealing time. The highest efficiency of 0.155% was achieved by the device utilising gold doped rGO annealed for 45 min. This is due to the device employing this sample possesses the smallest leak current.

**1. Introduction:** Carbon film has widely been utilised as counter electrode in dye-sensitised solar cell (DSSC) replacing costly platinum since it possesses high electronic conductivity, corrosion resistance, electrochemical reactivity and low cost [1, 2]. Graphene film can also be utilised as counter electrode of the device due to its excellent properties such as high conductivity and electrochemical stability [3–7]. Podlike N-doped carbon nanotubes encapsulating FeNi alloy nanoparticles was applied as counter electrode for DSSC and produced high efficiency of 8.82% [8]. Bismuth-based ternary nanowires, $Bi_{19}S_{27}Br_3$ was employed as efficient electrocatalysts for DSSC and yielded the efficiency of 8.70%. The efficiency was higher than that of the device utilising Pt counter electrode that was 7.99% [9]. In general, various materials have been utilised as counter electrode of DSSC such as carbon materials, conducting polymers, oxide and sulphide materials, transition-metal nitrides and carbides and composite materials [10].

In our previous work, reduced graphene oxide (rGO) was employed as counter electrode of DSSC [11]. The electrical property of rGO can be further improved by doping it with metal and non-metal. The performance of the DSSC can consequently be improved. Ju *et al.* [12] reported the use of nitrogen doped graphene films as superior counter electrode for DSSC. Wang *et al.* employed phosphorous doped rGO as counter electrode of DSSC [13]. The optical and electrical properties of doped rGO can be modified by varying the content of dopant, the annealing temperature and annealing time of doped rGO.

In this work, gold doped rGO synthesised by hummer method was employed as a counter electrode of DSSC. The originality of this work is the utilisation of gold doped rGO as counter electrode of the device. The goal of this work is to investigate the effect of annealing time of the sample on the performance parameters of the device.

## 2. Experimental

2.1. Preparation of gold doped rGO films: About 0.1 g GO powders were dissolved in 50 ml deionised water and the solution was sonicated for 1 h. About 2 mg gold (III) chloride trihydrate ($HAuCl.3H_2O$) powder equivalent to 2 wt% was then added into the solution and sonicated for 30 min. The solution was stirred for 5 min. The solution was finally spin coated three times on indium tin oxide (ITO) substrate at 1000 rpm for 15 s. The sample was annealed at 120°C in argon atmosphere for 15 min. These procedures were repeated by annealing the samples for 30, 45, 60, 75 and 90 min, respectively.

2.2. DSSC fabrication and performance study: The DSSC was fabricated by using gold doped rGO samples prepared for various annealing times as counter electrode. The $TiO_2$ films prepared on ITO substrate via liquid phase deposition technique was employed as photoanode of the device. The $TiO_2$ films were coated with N719 dye in ethanol solution for 15 h. About 0.5 M LiI/0.05 M $I_2$/0.5 M TBP in acetonitrile containing iodide/triiodide redox couple was used as a liquid electrolyte. A structure containing $TiO_2$ coated N719 film and gold doped rGO film was clamped in order to optimise the interfacial contact between these components. The electrolyte was injected into the structure via a capillary. The current–voltage ($I$–$V$) curves in dark and under illumination of 100 mW $cm^{-2}$ tungsten light were recorded by a Keithley high-voltage source model 237 interfaced with a personal computer. The illuminated area of the device was 0.23 $cm^2$. The electrochemical impedance spectroscopy (EIS) technique was also employed under illumination of 100 mW $cm^{-2}$ tungsten light to determine the bulk resistance ($R_b$), charge interfacial resistance ($R_{ct}$) and charge carrier lifetime at the applied voltage of 0.4 V.

**3. Results and discussion:** Fig. 1 depicts the $I$–$V$ curves in dark of the devices utilising the gold doped rGO counter electrode annealed for various times. It is noticeable that the dark current in forward bias is quite similar to that in reverse bias except for the device with the electrode annealed for 75 min. However for the device utilising 75 min sample, the forward bias current is higher than reverse bias current. Also, this device possesses the largest forward bias current compared with the other devices. This might be due to this device has the smallest bulk resistance as illustrated in Table 1. This means that the leak current is about the same with the forward bias current for other five devices. In other words, the devices do not possess rectification property. From the figure, it is noticed that the devices with the sample annealed for 15, 30, 45 and 60 min possess lower leak current than those of the devices with the samples annealed for 75 and 90 min. It can be said that the higher annealing times, the higher leak current. Higher leak current means higher recombination rate of electron hole. From these results, it is concluded that the dark current is influenced by the annealing time of gold doped rGO.




doi: 10.1049/mnl.2018.0054

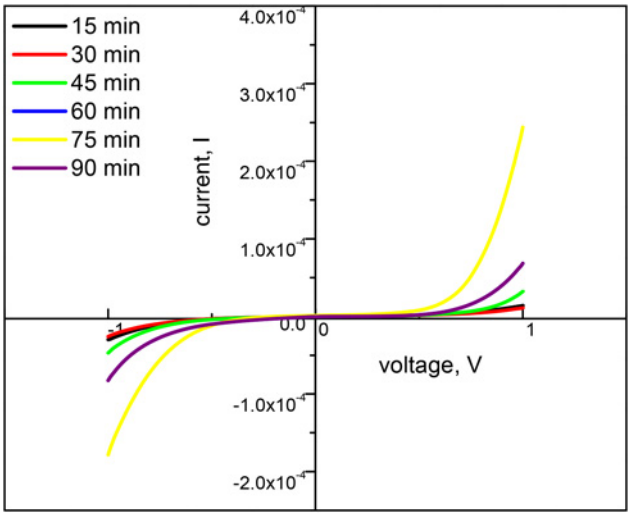


**Fig. 1** *Dark current of DSSC with various gold doped annealing times*

**Table 1** EIS parameters for DSSC with various annealing times

| Time, min | $R_b$, Ω | $R_{ct}$, Ω | $\tau$, ms |
|---|---|---|---|
| 15 | 330 | 1350 | 0.026 |
| 30 | 110 | 135 | 0.120 |
| 45 | 75 | 145 | 0.058 |
| 60 | 81 | 410 | 0.111 |
| 75 | 16 | 99 | 0.057 |
| 90 | 17 | 60 | 0.082 |

Fig. 2 shows the *J–V* curves under illumination of the devices utilising the samples annealed for various times. The device annealed for 15 min produces the lowest output power, followed by the devices utilising the samples annealed for 30, 60, 75, 90 and 45 min. The curve of the device with 15 min sample is represented by linear line, similar to the one reported by Rahman *et al.* [14]. The shape of the curve of the device with 30, 45 and 90 min samples is the same as that reported by Choi *et al.* [15]. The shape of the curve of the device utilising the sample annealed for 60 and 75 min follows the ideal curve of DSSC [16] or other types of solar cells such as silicon, thin film and organic solar cells. The photovoltaic parameters are analysed from the figure and illustrated in Table 2.

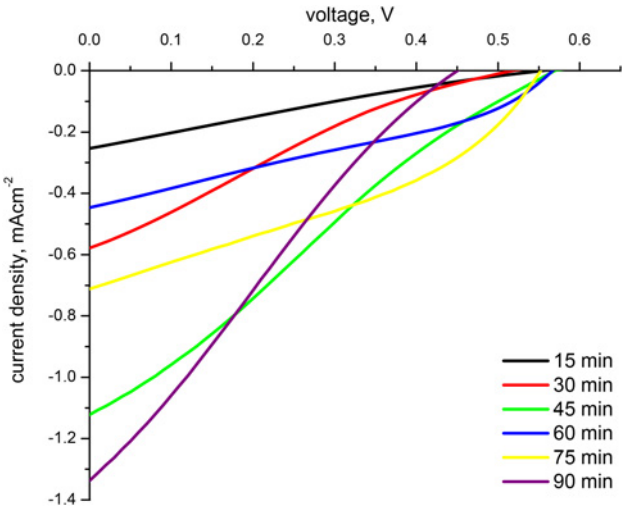


**Fig. 2** *J–V curves of DSSC with various gold doped rGO annealing times under 100 mW cm$^{-2}$ light illuminations*

From Table 2, it is noticed that the highest efficiency belongs to the device with 45 min sample. The device utilising 15 min sample demonstrates the lowest $J_{sc}$ and $\eta$. It is noticed from the table that the $J_{sc}$ and $\eta$ neither increase nor decrease with annealing time. The increase of power conversion efficiency can be related with the leak current and resistance of the device. The lower leak current results in the lower power loss in the device, consequently improves the power conversion efficiency. Also from Table 2, the $V_{oc}$ does not change significantly with annealing time. This is because $V_{oc}$ is only affected by the energy level of the components of the device such as energy gap of $TiO_2$ coated N719 dye, redox potential of the electrolyte and energy level of gold doped rGO. These energy levels are not affected by annealing time of gold doped rGO. In other words, $V_{oc}$ is not affected by the properties of gold doped rGO. While, according to the table, the *FF* is low since the slope of the *J–V* curves is high as shown in Fig. 2. Generally, the best efficiency of 0.155% is low since the device utilises platinum-free counter electrode that is gold doped rGO. The DSSC utilising platinum counter electrode performed higher efficiency than that of the device employing non-platinum counter electrode [16]. The highest efficiency of this work was found to be much lower than that of the DSSC utilising nitrogen doped graphene and phosphorous doped rGO counter electrode, respectively [12, 13]. The efficiency of the DSSC utilising nitrogen doped graphene and phosphorous doped rGO were 9.05 and 6.25%, respectively. This is due to the $R_{ct}$ of the device fabricated in this work that is 145 Ω is much larger than that reported in [12, 13] that were 1.73 and 3.28 Ω, respectively.

Fig. 3 depicts the Nyquist plots of the device with various gold doped rGO annealing times. The impedance spectra for the device utilising 15 and 60 min samples show three semi-circles for which the smallest semi-circle represents the bulk resistance ($R_b$), the middle semicircle denotes the charge transfer resistance at the interface $TiO_2$-N719 dye/electrolyte ($R_{ct1}$) and the biggest one indicates the charge transfer resistance at the interface electrolyte/gold doped rGO electrode ($R_{ct2}$). The other four devices display two semicircles. The $R_b$ and $R_{ct}$ are estimated from the real impedance ($Z$) and illustrated in Table 1. These EIS data can also be used to explain the photovoltaic parameters listed in Table 2.

Fig. 4 depicts the Bode plots of the device with various annealing times. Two peaks appear in the plots belonging to the device with 15, 60 and 90 min samples. The plots of the device with 30, 45 and 75 min samples display one peak. However, the highest peak representing resonant frequency of each device is used to calculate the carrier lifetime. The carrier lifetimes are presented in Table 1. Carrier lifetime is defined as the time taken by the charge carrier which is electron to travel across the interface of $TiO_2$-N719 dye before recombining with hole at the interface of electrolyte/gold doped rGO. According to the table, the device utilising the sample annealed for 15 min possesses the shortest lifetime and the device with 30 min has the longest lifetime.

According to Table 1, the device utilising the 75 min sample demonstrates the lowest $R_b$ while the device employing 90 min sample possesses the smallest $R_{ct}$. However, according to Table 2, the device with 45 min sample performs the highest $\eta$. According to Table 1, the device with 45 min sample just possesses the third lowest $R_b$ and $R_{ct}$. From Table 1, the $\eta$ of the device with 75 and 90 min sample is lower than that of the device with 45 min sample. This might be due to the device utilising 75 and 90 min samples have lower dye loading than that of the device with 45 min samples. It is found that from Table 2, the device with 90 min samples yields the highest $J_{sc}$ which might be due to the lowest $R_{ct}$.

**Table 2** Photovoltaic parameters for DSSC with various annealing times

| Time, min | $J_{sc}$, mA cm$^{-2}$ | $V_{oc}$, V | *FF* | $\eta$, % |
|---|---|---|---|---|
| 15 | 0.258 ± 0.006 | 0.551 ± 0.007 | 0.221 ± 0.008 | 0.031 ± 0.008 |
| 30 | 0.588 ± 0.004 | 0.511 ± 0.005 | 0.109 ± 0.004 | 0.064 ± 0.004 |
| 45 | 1.134 ± 0.003 | 0.561 ± 0.003 | 0.243 ± 0.002 | 0.155 ± 0.001 |
| 60 | 0.452 ± 0.001 | 0.561 ± 0.003 | 0.324 ± 0.004 | 0.082 ± 0.003 |
| 75 | 0.712 ± 0.006 | 0.550 ± 0.001 | 0.371 ± 0.002 | 0.146 ± 0.008 |
| 90 | 1.358 ± 0.007 | 0.440 ± 0.005 | 0.240 ± 0.004 | 0.143 ± 0.001 |

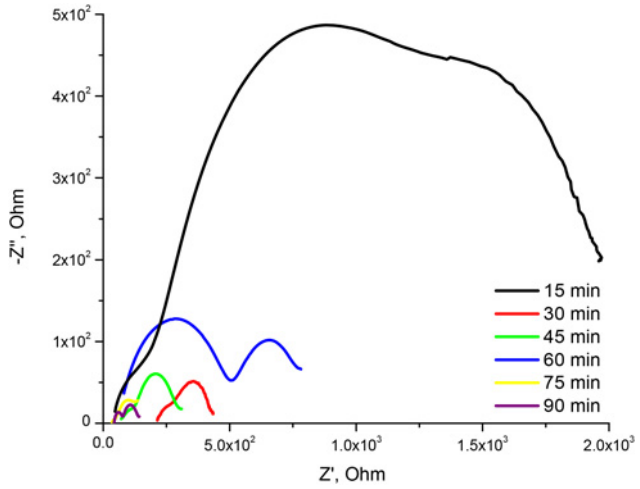


**Fig. 3** *Nyquist plots with various gold doped rGO annealing times under 100 mW cm$^{-2}$ light illuminations*

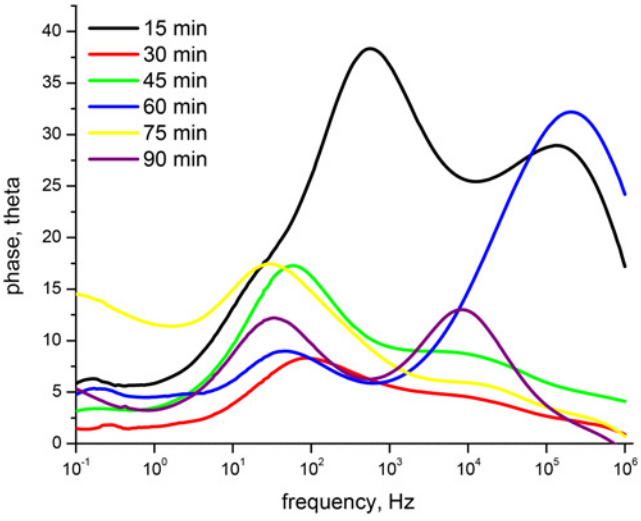


**Fig. 4** *Bode plots with various gold doped rGO annealing times under 100 mW cm$^{-2}$ light illuminations*

**4. Conclusions:** Gold doped rGO film has successfully been prepared and employed as counter electrode of DSSC. The device applying the sample annealed at 120°C for 45 min demonstrates the highest power conversion efficiency of 0.155%. This is due to the device utilising the sample annealed for 45 min has the lowest leak current.

**5. Acknowledgment:** This work was supported by Universiti Kebangsaan Malaysia (UKM) under research grant no. GUP-2016-013.

## 6 References

[1] Huang Z., Liu X., Li K., *ET AL.*: 'Application of carbon materials as counter electrodes of dye-sensitized solar cells', *Electrochem. Commun.*, 2007, **9**, pp. 596–598
[2] Nam J.G., Park Y.J., Kim B.S., *ET AL.*: 'Enhancement of the efficiency of dye-sensitized solar cell by utilizing carbon nanotube counter electrode', *Scr. Mater.*, 2010, **62**, pp. 148–150
[3] Zhang D.W., Li X.D., Li H.B., *ET AL.*: 'Graphene-based counter electrode for dye-sensitized solar cells', *Carbon*, 2011, **49**, pp. 5382–5388
[4] Wang H., Sun K., Tao F., *ET AL.*: '3D honeycomb-like structured graphene and its high efficiency as a counter-electrode catalyst for dye-sensitized solar cells', *Angew. Chem. Int. Ed.*, 2013, **52**, pp. 9210–9214
[5] Kavan L., Yum J.-H., Grätzel M.: 'Graphene-based cathodes for liquid-junction dye sensitized solar cells: electrocatalytic and mass transport effects', *Electrochim. Acta*, 2014, **128**, pp. 349–359
[6] Janani M., Srikrishnarka P., Nair S.V., *ET AL.*: 'An in-depth review on the role of carbon nanostructures in dye-sensitized solar cells', *J. Mater. Chem. A*, 2015, **3**, pp. 17914–17938
[7] Kavan L., Liska P., Zakeeruddin S.M., *ET AL.*: 'Low-temperature fabrication of highly-efficient, optically-transparent (FTO-free) graphene cathode for co-mediated dye-sensitized solar cells with acetonitrile-free electrolyte solution', *Electrochim. Acta*, 2016, **195**, pp. 34–42
[8] Xiaojia Z., Jiao D., Nan W., *ET AL.*: 'Podlike N-doped carbon nanotubes encapsulating FeNi alloy nanoparticles: high-performance counter electrode materials for dye-sensitized solar cells', *Angew. Chem. Int. Ed.*, 2014, **53**, pp. 7023–7027
[9] Yihui W., Bin Z., Chi Y., *ET AL.*: 'Bismuth-based ternary nanowires as efficient electrocatalysts for dye sensitized solar cells', *Chem. Commun.*, 2017, **53**, pp. 5445–5448
[10] Jayaraman T., Arumugam R.S., Jayannathan M., *ET AL.*: 'Recent progress in non-platinum counter electrode materials for dye-sensitized solar cells', *Chem. Electro. Chem.*, 2015, **2**, pp. 928–945
[11] Rahman M.Y.A., Sulaiman A.S., Umar A.A., *ET AL.*: 'Dye-sensitized solar cell (DSSC) utilizing reduced graphene oxide (RGO) films counter electrode: effect of graphene oxide (GO) content', *J. Mater. Sci., Mater. Electron.*, 2017, **28**, pp. 1674–1678
[12] Ju M.J., Kim J.C., Choi H.-J., *ET AL.*: 'N-doped graphene nanoplatelets as superior metal-free counter electrodes for organic dye-sensitized solar cells', *ACS Nano*, 2013, **6**, pp. 5243–5250
[13] Wang Z., Li P., Chen Y., *ET AL.*: 'Phosphorus-doped reduced graphene oxide as an electrocatalyst counter electrode in dye-sensitized solar cells', *J. Power Sources*, 2014, **263**, pp. 246–251
[14] Rahman M.Y.A., Salleh M.M., Talib I.A., *ET AL.*: 'Current transport mechanism and photovoltaic properties of photoelectrochemical cells of ITO/$TiO_2$/PVC–$LiClO_4$/graphite', *Curr. Appl. Phys.*, 2007, **7**, pp. 446–449
[15] Choi H., Kim H., Hwang S., *ET AL.*: 'Dye-sensitized solar cells using graphene-based carbon nano composite as counter electrode', *Sol. Energy Mater. Sol. Cells*, 2011, **95**, pp. 323–325
[16] Sulaiman A.S., Rahman M.Y.A., Umar A.A., *ET AL.*: 'Dye-sensitized solar cell (DSSC) utilizing $TiO_2$ nanostructure films: effect of synthesis temperature', *Russ. J. Electrochem.*, 2018, **54**, pp. 56–61




doi: 10.1049/mnl.2018.0054